

Fluorenone-Containing Polyfluorenes and Oligofluorenes: Photophysics, Origin of the Green Emission and Efficient Green Electroluminescence[†]

Abhishek P. Kulkarni, Xiangxing Kong, and Samson A. Jenekhe*

Department of Chemical Engineering and Department of Chemistry, University of Washington, Seattle, Washington 98195-1750

Received: October 15, 2003; In Final Form: April 17, 2004

A series of four new statistical copolymers of 9,9-dihexylfluorene and 9-fluorenone with well-defined structures and a new fluorene–fluorenone–fluorene trimer model compound were synthesized and used to investigate the photophysics, origin of the green emission, and electroluminescence of this class of light-emitting materials. We show that the new oligofluorene trimer with a central fluorenone moiety is an excellent model of the green-emitting chromophore in polyfluorenes. From systematic studies of the steady-state photoluminescence (PL) and PL decay dynamics of solutions of the fluorenone-containing copolymers and oligomer and thin films of the copolymers, we show that the controversial 535-nm green emission band originates from the fluorenone defects in single-chain polyfluorenes and not from intermolecular aggregates or excimers. The green emission, centered at 535 nm, was observed in dilute toluene solutions of all fluorenone-containing copolymers and oligomer; it was long-lived with a single-exponential PL lifetime of ~ 5 ns, compared to a lifetime of 240–400 ps for the blue emission. The PL decay dynamics of the 535-nm emission from thin films of all copolymers was also well-described by a single-exponential lifetime of 5–6 ns. The observed increased intensity of the green emission with increased intermolecular interactions in solution or solid state can be explained by the increased excitation energy transfer from fluorene segments to the fluorenone moieties. Bright green electroluminescence (EL) centered at 535 nm was achieved from single-layer copolymer light-emitting diodes (LEDs), ITO/PEDOT/copolymer/Al, with luminances of 1600–3340 cd/m² that varied with fluorenone content. The EL data suggest that the fluorene–fluorenone copolymers are very promising materials for green LEDs.

Introduction

Electroluminescent devices based on organic and polymer semiconductors are promising for applications in displays and lighting.^{1–3} Among the many classes of electroluminescent polymers under current investigation, the polyfluorenes have emerged as attractive blue light-emitting materials with high photoluminescence quantum yields in the solid state^{3a,b} and high hole mobility.⁴ However, a major problem that is involved with the use of poly(9,9-dialkylfluorene)s as blue-emitting materials in light-emitting diodes (LEDs) is the undesirable lower-energy emission band centered at 530–540 nm that appears under device operation, turning the pure blue emission to a blue-green color.^{3a,b} Although many approaches to stabilize the pure blue emission from the polyfluorenes have been explored, the origin of the additional green emission band has been controversial and remains not fully understood.⁵

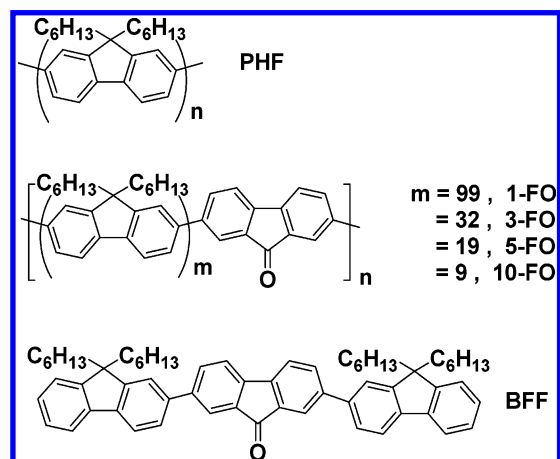
So far, different models have been proposed to explain the origin of the green emission; however, none has yet conclusively resolved the exact nature of the emission. Initial assignment of the green emission band of the polyfluorenes to aggregate emission was based on prior observations on related ladder poly(*p*-phenylene)s.^{6a} It was, however, later assigned to emission from intermolecular excimers presumably formed by the more planar fluorenone moieties produced by photo-/electro-oxidation at the 9-fluorene sites of the polymer chains.^{6b}

Various approaches, including addition of bulky side groups,^{5a,b} bulky end groups,^{5c} copolymerization,^{5d} dendronization,^{5e} and blending,^{5f,g} were thus explored for minimizing intermolecular interactions and, hence, for stabilizing the blue emission of the polyfluorenes. These approaches have succeeded to varying degrees. However, a new hypothesis was recently made, claiming that emission from isolated fluorenone defects on polyfluorene chains, rather than intermolecular aggregates or excimers, is responsible for the green emission band. It was proposed that these fluorenone defects could be formed either during polymerization or later by thermal or photo-oxidation of polyfluorene films.^{6c–e} The main evidence for this hypothesis was the observation of the green emission band in very dilute solutions of the fluorene oligomers and polymers^{6d} and fluorenone-containing copolymers,^{6e} the lack of any significant concentration dependence of the green emission band in solutions of fluorenone-containing copolymers, and the pronounced vibronic structure of the green emission band from thin films of fluorenone–fluorene copolymers at low temperatures.^{6e} Recent results from time-gated electroluminescence (EL) spectroscopy of polyfluorene LEDs have shown that the contribution of the green emission band, relative to the blue, increased as the delay time increased, and this phenomenon has been attributed to the delayed recombination of charge carriers on the on-chain low-energy fluorenone defects, which act as deep electron traps.^{6f,g} In addition, some recent theoretical studies on model fluorenone-containing oligomers have shown that the green emission

[†] Part of the special issue “Alvin L. Kwiram Festschrift”.

* Author to whom correspondence should be addressed. E-mail: jenekhe@u.washington.edu.

CHART 1



originates from the fluorenone moieties due to very efficient energy transfer and strong localization of the excitons on the low-energy fluorenone units.⁷

The notion that keto defects, in the form of fluorenone moieties, are formed in polyfluorene thin films by photo/electro-oxidation has overwhelming experimental evidence in the literature.^{6b,c} However, the fact that 9-fluorenone moieties are more planar than 9,9-dialkylfluorene units is one reason fluorenone-containing polyfluorenes may be more prone to aggregation and excimer formation than the defect-free polyfluorene chains. This complicates the situation, because it is very likely then that the origin of the green emission could be the isolated fluorenone moieties and/or the aggregates/excimers of fluorenone moieties on the polymer chains. Prior studies of copolymers of 9,9-dialkylfluorene and 9-fluorenone have thus led to opposite conclusions regarding the origin of the green emission band.⁸ Dilute solution and solid-state photophysical investigation of random copolymers of 9-fluorenone and 9,9-dinonylfluorene that contain 1, 5, 10, and 20 wt % of fluorenone claimed that the origin of the green emission band was excimers and/or aggregates based on short fluorenone segments in the copolymer chains.^{8b} On the other hand, recent studies on statistical copolymers of 9-fluorenone and 9,9'-difarnesylfluorene propose that the green emission originates from on-chain emissive keto defects, because the green emission band was observed even in very dilute solutions of the fluorenone-containing copolymers and showed no concentration dependence in solution, unlike an aggregate or excimer emission.^{6c} So far, no clear verdict has been made on the exact nature of the controversial green emission band in polyfluorenes. However, it is vital to understand the exact origin of the green emission, because this would dictate the future methodologies, both synthetic and device fabrication-related, of stabilizing the blue emission and paving the way for commercial realization of blue and full-color polymer LEDs.

In this paper, we report studies of the photophysics, the origin of the green emission, and EL of a series of new fluorenone-containing poly(9,9-dihexylfluorene)s (PHFs). Unlike previously investigated fluorene-fluorenone copolymers that were made by Yamamoto coupling reactions of dibromides, the present statistical copolymers were synthesized by Suzuki coupling polymerization, which ensured achievement of the well-defined molecular structures shown in Chart 1. Thus, each 9-fluorenone moiety was isolated within the PHF chains. A series of four copolymers that contain 1, 3, 5, and 10 mol % fluorenone, denoted 1-FO, 3-FO, 5-FO, and 10-FO (Chart 1), respectively, was investigated. To understand further the chromophore

involved in the green emission band, we have also synthesized 2,7-bis(2'-9',9'-dihexylfluorenyl)-9-fluorenone (BFF), which is a trimer oligofluorene with one central fluorenone ring whose structure is shown in Chart 1, and investigated the solution photophysics. In our view, this compound is a better representation of the lowest-energy chromophore in the fluorenone copolymers than 9-fluorenone molecule. Interestingly, this particular model compound and other related fluorenone-containing oligofluorenes have previously been theoretically investigated but not experimentally.⁷ The photophysics was investigated by optical absorption, steady-state photoluminescence (PL), time-resolved PL decay dynamics, and PL quantum yield measurements. Bright green EL was obtained from all the copolymers, which demonstrates that, although the fluorenone defects in the polyfluorenes completely destroy the normal blue emission, they can instead be used as efficient green electroluminescent materials in LEDs.

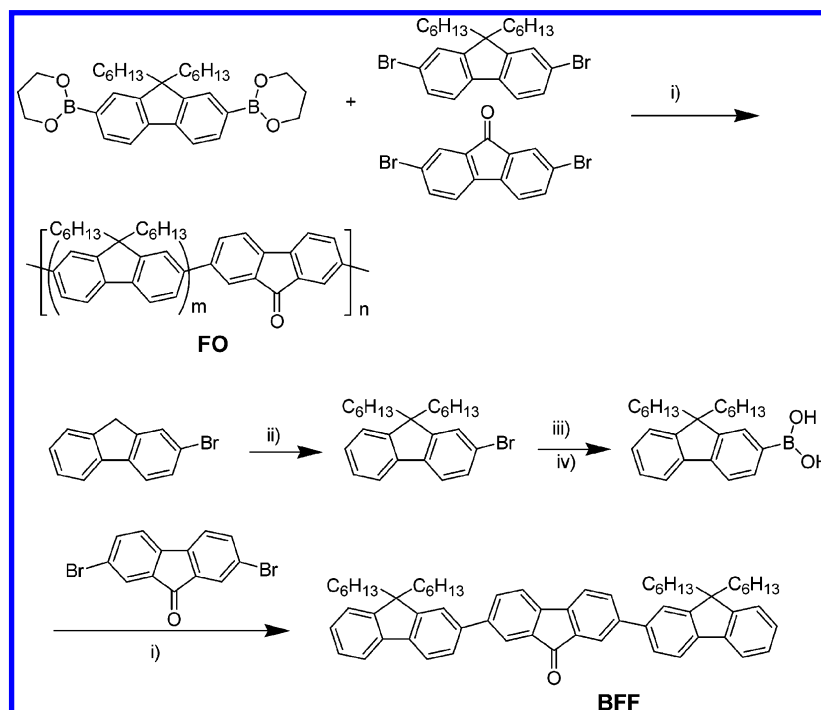
Results and Discussion

Synthesis and Characterization of Copolymers. The poly-(9,9-dihexylfluorene-co-fluorenone)s with fluorenone fractions of <50 mol % were synthesized by Suzuki coupling polymerization (Scheme 1). The molar ratio of fluorenone moiety in the copolymers was controlled by adjusting the molar ratio between 9,9-dihexyl-2,7-dibromofluorene and 2,7-dibromofluorenone while maintaining a 1/1 molar ratio between the dibromides and the bis(trimethylene boronate). The copolymers were purified twice by precipitation from THF solution into methanol/HCl (100/1, v/v). The colors of the copolymers were light yellow for 1-FO, yellow for 3-FO, 5-FO and 10-FO, and orange for 50-FO. All the fluorene-fluorenone copolymers were soluble in organic solvents such as chloroform, toluene, and tetrahydrofuran (THF), except 50-FO, which was insoluble in these solvents. The copolymers have number-average molecular weights (gel permeation chromatography (GPC), polystyrene calibration) of $M_n = 21\,700\text{--}36\,400$, as shown in Table 1. The number-average degree of polymerization was $DP_n = 65\text{--}110$.

The synthesis of the model compound BFF, by Suzuki coupling, is also shown in Scheme 1. Figure 1 shows the Fourier transform infrared (FT-IR) spectra of the model compound BFF, along with the 5-FO and 10-FO copolymers. Two main vibrational bands located at 1718 and 1448 cm^{-1} are characteristic of the C=O stretch in the fluorenone moiety and the aromatic C=C, respectively.^{8b} The peak at 1606 cm^{-1} is related to the fluorenone moiety and assigned to a stretching mode of an asymmetrically substituted benzene.^{6b} The relative intensity of the keto vibration band at 1718 cm^{-1} increased as the fluorenone amount in the copolymers increased. The structures of the copolymers and the model compound BFF were also confirmed by ^1H NMR spectra. The ^1H NMR spectra of 10-FO and BFF and their assignment, shown in Figure 2, are consistent with the proposed structures. A small peak at 8.03 ppm due to the aromatic proton adjacent to the keto group in fluorenone was observed in the spectra of 5-FO and 10-FO; however, this peak was not observed in the spectra of 3-FO and 1-FO, because of the low concentration of fluorenone moiety. Unlike the copolymers, BFF shows multiple peaks at $7.2\text{--}7.4\text{ ppm}$, which are assigned to the aromatic protons of the terminal fluorene.

The thermal properties of the copolymers were evaluated by thermogravimetric analysis (TGA) and differential scanning calorimetry (DSC) under a nitrogen atmosphere. TGA revealed that all the copolymers are thermally stable up to $380\text{ }^\circ\text{C}$ (<1% weight loss). The weight loss at $600\text{ }^\circ\text{C}$ decreased as the

SCHEME 1



(i) $\text{Pd}(\text{PPh}_3)_4$, Aliquat 336, 2 M Na_2CO_3 toluene. (ii) 1-bromohexane, KOH, DMSO/ H_2O . (iii) BuLi, THF, -78°C , $(\text{CH}_3\text{O})_3\text{B}$. (iv) 2 M HCl.

TABLE 1: Molecular Weights and Thermal Properties of Fluorene-Fluorenone Copolymers

sample	fluorenone fraction (%, mol/mol)	M_n^a ($\times 10^4$)	M_w/M_n^a	DP_n^b	T_g ($^\circ\text{C}$)	T_d ($^\circ\text{C}$)
1-FO	1	2.76	2.68	83	105	380
3-FO	3	2.17	2.26	65	106	380
5-FO	5	3.64	3.39	110	108	380
10-FO	10	3.35	3.33	101	118	380

^a Measured by gel permeation chromatography (GPC), using PSt standards. ^b Degree of polymerization; $\text{DP}_n = M_n/M_{\text{DHF}}$.

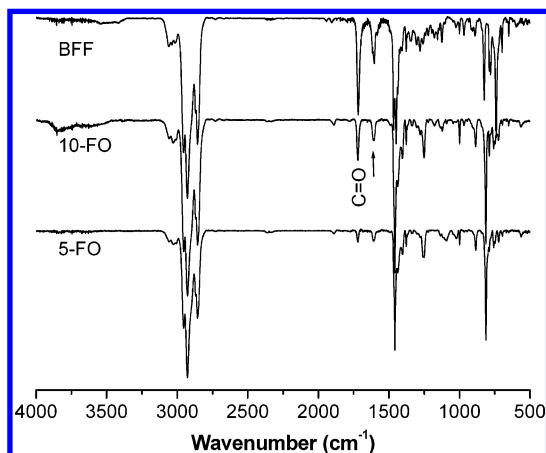


Figure 1. FT-IR spectra of 5-FO and 10-FO copolymers and model compound BFF.

fluorenone fraction increased, suggesting that the weight loss is caused by decomposition of the hexyl side groups. As shown in Figure 3, three of the copolymers showed glass transitions at 105–108 $^\circ\text{C}$, whereas 10-FO had a slightly higher glass transition at 118 $^\circ\text{C}$. Besides, 1-FO showed a melting transition at 240 $^\circ\text{C}$, which was not observed in the other copolymers. The PHF homopolymer is known to have a glass transition temperature of $T_g \approx 94^\circ\text{C}$, a liquid crystalline phase transition

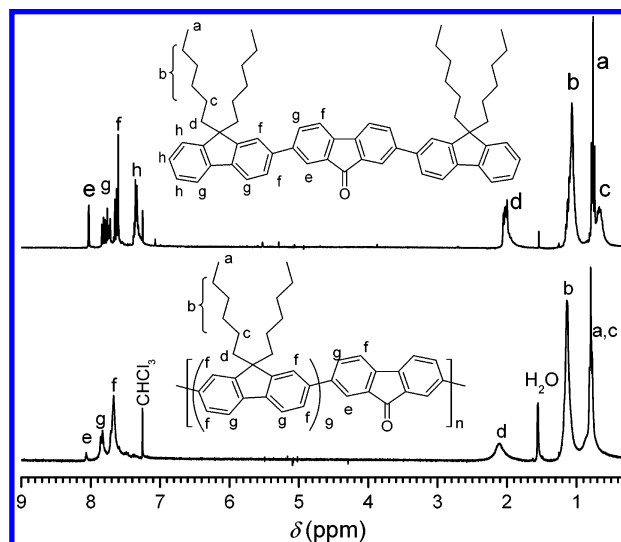


Figure 2. ^1H NMR spectra of model compound BFF and copolymer 10-FO.

at ~ 160 – 240°C , and a melting point at 290 – 300°C .⁹ The existence of rigid, planar, fluorenone moieties in the polyfluorenes thus affects thermal properties, as seen with the relatively higher glass transitions and the absence of clear melting transitions in the copolymers that contain higher fractions of fluorenone.

Steady-State Photophysics in Solution. One of the objectives of the photophysical investigation of the fluorenone copolymers is to determine whether the undesirable green emission in polyfluorenes is from aggregates, excimers, or fluorenone sites on single chains. Figure 4a shows the optical absorption spectra of dilute (10^{-6} M) toluene solutions of the PHF homopolymer and the four fluorenone copolymers. The absorption maxima of all four copolymers are located at 382 nm and that of PHF is located at 388 nm. This band is associated with the π – π^* transition of the polyfluorene backbone. An increase in the fluorenone content leads to a slight increase in

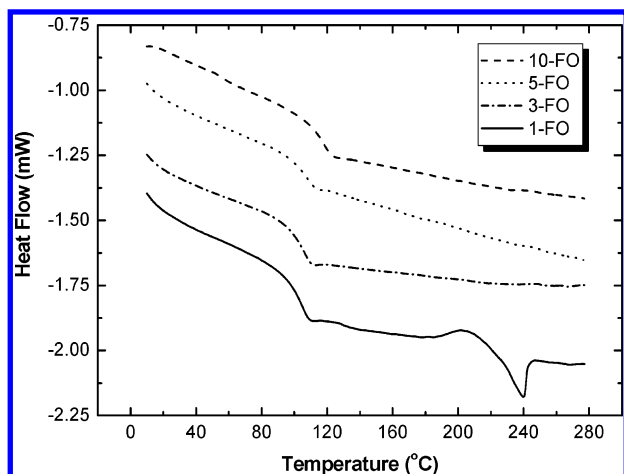


Figure 3. Second heating DSC curves of fluorene-fluorenone copolymers with a heating rate of 10 °C/min in nitrogen.

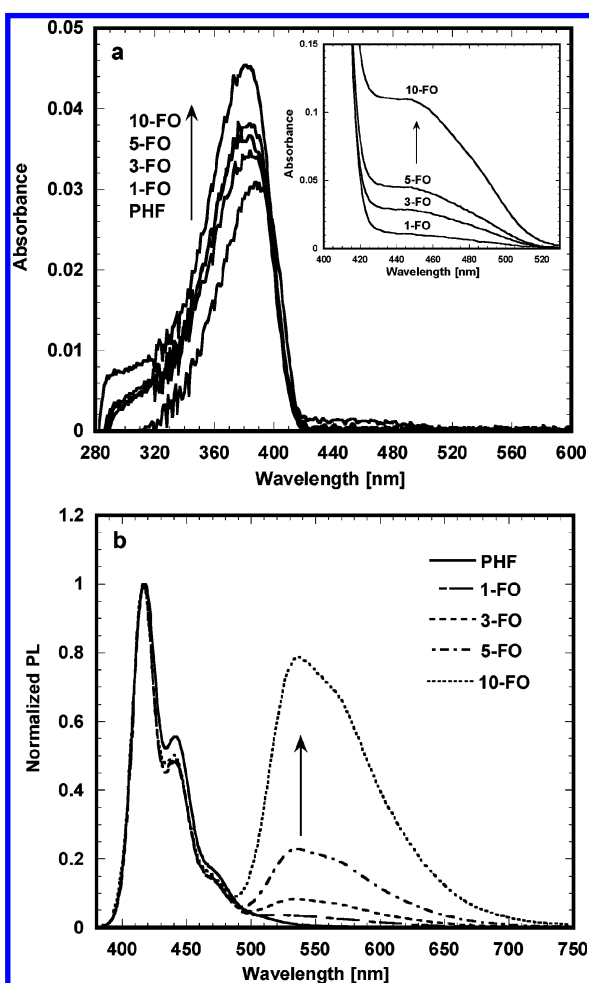


Figure 4. (a) Optical absorption spectra of 10^{-6} M solutions of PHF and fluorenone copolymers in toluene. Inset shows the absorption spectra of 10^{-4} M solutions of the same copolymers. (b) Normalized PL emission spectra of 10^{-6} M solutions of the polymers in toluene under 380-nm excitation.

the absorption at 450 nm. However, because of the low concentration of fluorenone, this absorption band at 450 nm is not well-resolved at 10^{-6} M. It is clearer in the absorption spectra of 10^{-4} M solutions, as shown in the inset of Figure 4a. A distinct growth in the 450-nm band is observed as the fluorenone fraction increases from 1-FO to 10-FO. This low oscillator strength band is associated with the $n-\pi^*$ transition of fluorenone.^{7a}

The photoluminescence (PL) emission spectra of the polymers in toluene solutions (10^{-6} M), normalized relative to the blue peak, are shown in Figure 4b. The PL spectrum of PHF exhibits two well-resolved peaks at 416 and 440 nm, with the 0–0 transition at 416 nm being the dominant one.^{3a} In addition to these two peaks, the emission spectra of the copolymers have a third band at 535 nm. This additional band grows in intensity with increasing fluorenone content from 1-FO to 10-FO and is fixed at 535 nm in all four copolymers. In the case of 10-FO, this 535-nm green band is almost 80% as intense as the blue band at 416 nm. This 535-nm emission band matches exactly with the previously reported troublesome green EL band in blue-emitting polyfluorenes.^{3a,b} The fact that this emission is seen in such dilute copolymer solutions suggests that it does not originate from intermolecular aggregates or excimers. It is clearly related to the fluorenone moieties in isolated chains, because the relative intensity of the green emission band increases as the fluorenone content in the copolymer increases.

Both aggregate and excimer emissions in solution display a strong concentration dependence, because they are interchain phenomena. We thus investigated the PL emission of all polymers in toluene solution at three different concentrations of 10^{-7} , 10^{-6} , and 10^{-4} M. The concentration-dependent PL emission spectra of PHF, 3-FO, and 10-FO, normalized relative to the blue peak, are shown in Figure 5. The PHF spectra shown in Figure 5a have no green emission band at any concentration. The only difference in the PL spectra of PHF is that the spectrum of the 10^{-4} M solution is red-shifted by 6 nm, compared to the more dilute solutions. However, the PL spectra of 3-FO (Figure 5b) show a steady growth in the 535-nm band as the solution concentration increases. The effect is most dramatic for 10-FO, as shown in Figure 5c, where the 535-nm green band is more intense than the blue emission band at a concentration of 10^{-4} M. A similar concentration dependence of the 535-nm band was also observed for solutions of 1-FO and 5-FO (spectra not shown). These results suggest that as the degree of intermolecular interactions in solution increases with concentration from 10^{-7} M to 10^{-4} M, the green emission from the fluorenone defects is enhanced. We note that Romaner et al. did not observe such a concentration dependence of the green emission band in toluene solutions of polyfluorenes that contained fluorenone defects.^{6c} However, the range of solution concentrations they studied ($\sim 10^{-8}$ – 10^{-7} M) was much smaller than the present study. Nonetheless, it is not possible to conclude whether the green emission band is from an excimer solely from these PL spectra. It is well-known that excimer formation drastically reduces the PL quantum yield (ϕ_f), because of the greater number of nonradiative decay pathways for depopulation of the excited state.¹⁰ For the present copolymer solutions, we observed a steady decrease in ϕ_f with increasing solution concentration. In addition, the ϕ_f decreases as the amount of fluorenone in the copolymer increases. The estimated fluorescence quantum yields of the polymers in 10^{-6} M solutions were $\phi_f = 1, 0.98, 0.77, 0.47$, and 0.29 for PHF, 1-FO, 3-FO, 5-FO, and 10-FO, respectively. This observation is consistent with the theoretical claims that fluorescence quantum efficiencies of fluorenone-containing materials are usually low.^{7a} The observed strong concentration dependence of the green emission band in solution suggests that increased interchain interactions among the fluorenone-containing polyfluorene chains enhance the emission from the fluorenone defects.

The absorption and PL emission spectra of 10^{-4} M solutions of BFF in moderately polar toluene and highly polar acetonitrile are shown in Figure 6a. The absorption spectra are identical in

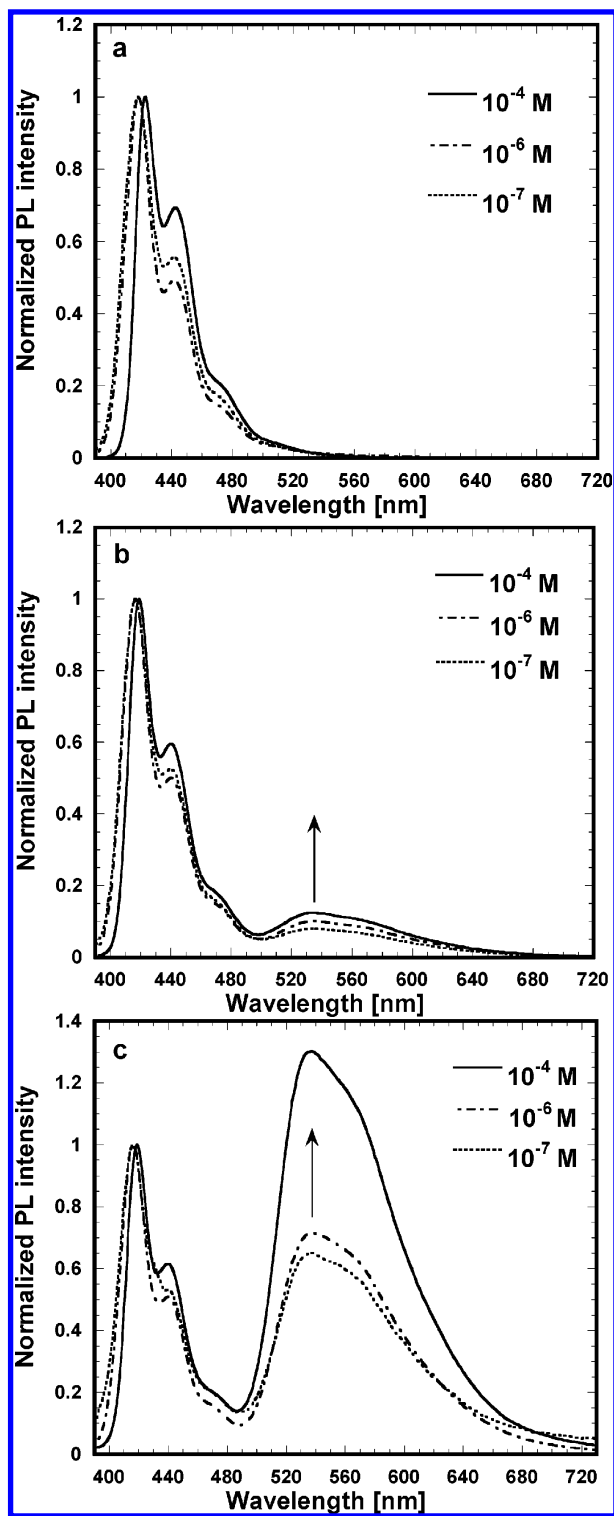


Figure 5. Normalized PL emission spectra of polymer solutions in toluene at different concentrations under 380-nm excitation: (a) PHF, (b) 3-FO, and (c) 10-FO.

both solvents, with two peaks at 352 and 311 nm, in addition to a broad band at 450 nm. Comparing these experimental spectra to previous theoretical results, the transition at 352 nm probably corresponds to the singlet state S_3 , and the peak at 450 nm corresponds to the S_1 ($n-\pi^*$) state because it has a very low oscillator strength ($\epsilon \approx 250 \text{ M}^{-1} \text{ cm}^{-1}$).^{7a} Compared to the absorption spectra of the fluorenone-fluorene copolymers in solution (Figure 4a), the absorption maxima of BFF at 352 nm is blue-shifted from the 382 nm value observed in the

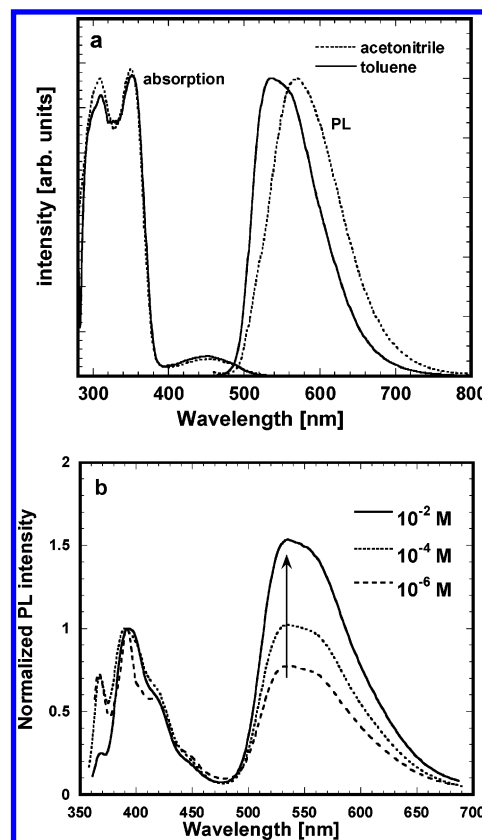


Figure 6. (a) Absorption and PL emission spectra of 10^{-4} M solution of BFF in toluene and acetonitrile. The excitation wavelength was 450 nm. (b) Normalized PL emission spectra of BFF in toluene at different concentrations under 350-nm excitation.

copolymers, as expected. However, the transition at 450 nm is observed in the absorption spectra of BFF and the fluorenone copolymers, implying that it is independent of chain length. This observation is consistent with theoretical results, showing that the energy of the S_1 ($n-\pi^*$) state in all fluorenone-containing oligofluorenes is fixed.^{7a} The PL emission spectra of BFF on selective excitation at 450 nm show a broad emission band with maxima at 535 nm in toluene, which is exactly the same as the emission spectra of the fluorenone copolymers in toluene previously shown in Figure 4b. However, the PL emission maximum of BFF in acetonitrile is red-shifted by 35 nm, to 570 nm, indicating a strong polar character of the excited-state species due to the presence of the carbonyl bridge in the fluorenone moiety.

Similar to the concentration-dependent PL spectra of the fluorenone copolymers in solution, we investigated the PL emission of BFF in solution at three different concentrations to probe the effects of intermolecular interactions. The PL emission spectra of BFF for 350-nm excitation, normalized relative to the blue peak at 393 nm, are shown in Figure 6b for 10^{-6} , 10^{-4} , and 10^{-2} M toluene solutions. We identify two or three sharp vibronic peaks below 440 nm, which are reminiscent of typical small molecule monomer emission spectra.^{10c} The green emission band at 535 nm steadily grows as the solution concentration increases, finally becoming 1.5 times greater than the intensity of the blue band at 393 nm in the 10^{-2} M solution. This indicates that there is a clear role of intermolecular interactions in the evolution of the green band in BFF, similar to the emission of fluorenone copolymer solutions. In addition, the PL quantum yields decrease as the BFF concentration increases and are generally low (19% for 10^{-6} M toluene solution), as expected for small aromatic ketones.^{10c} These results confirm that the

trimer model compound BFF is an excellent model of the chromophore that causes the green emission in the fluorenone copolymers. The discussion so far has dealt with solution photophysics from which we have ruled out the possibility that the green emission band originates from aggregates. To decide whether the emission is from a single-chain or interchain species, we now discuss the photophysics in the solid state where the degree of interchain interactions is at its maximum.

Steady-State Photophysics in Solid State. The optical absorption spectra of thin films of PHF and the fluorenone copolymers are shown in Figure 7a. The absorption maxima of all the polymers are located at 382 ± 1 nm, almost identical to that in dilute solution (Figure 4a), and correspond to the singlet $\pi-\pi^*$ transition of the polyfluorene backbone. With an increase in fluorenone content from 1-FO to 10-FO, there is a slight increase in the absorption feature at ~ 450 nm. This is to be compared to the growth in the 450-nm absorption band of the copolymers in 10^{-4} M toluene (see inset of Figure 4a). This absorption band is associated with the fluorenone moiety and is weak because of the low concentration of fluorenones in the copolymers and the low oscillator strength of the first two singlet transitions of fluorenone.^{7a}

The PL emission spectra of the polymer thin films, normalized relative to the dominant green emission band, are shown in Figure 7b for 380-nm excitation. The PHF spectrum shows pure blue emission with two vibronic peaks at 428 and 449 nm and is slightly red-shifted compared to its dilute solution PL spectrum. On the other hand, all fluorenone copolymer thin films emit green light, with dominant emission bands centered at 534–546 nm. The blue emission is substantially quenched and is steadily decreased as the fluorenone content in the copolymers increased. With just 1 mol % of fluorenone (1-FO), the blue band is already quenched, such that it is only 20% of the intensity of the green band, whereas the blue emission is barely discernible in the emission spectrum of 10-FO thin film. Besides, the PL maxima of the green emission band progressively red-shifts from 534 nm to 539 nm to 542 nm to 546 nm for 1-FO, 3-FO, 5-FO, and 10-FO thin films, respectively. It was shown that, compared to pure oligofluorenes, the energy of the $\pi-\pi^*$ transition is lower in the oligofluorenes that contain fluorenone units.^{7a} It was thus proposed that the green emission band from that transition would shift to longer wavelengths as the number of fluorenone units on the polyfluorene chains increases,^{7a} which explains the red-shift in the emission maxima that is observed experimentally here. These thin-film emission spectra are quite similar to the previously discussed dilute solution emission spectra of fluorenone-containing polyfluorenes. As the degree of intermolecular interactions increases in going from dilute solution to thin film, the green emission becomes dominant, relative to the blue. Such dominant green emission has been reported for fluorenone-containing polyfluorenes^{6c} and poly-(fluorenyleneethynylene)s¹¹ and explained as being due to efficient energy transfer to the lower-energy fluorenone sites.

Figure 7c shows the PL emission spectra of the fluorenone copolymer thin films, normalized relative to the blue peak at 424 nm. The ratio of green:blue emission is 5:1, 18:1, 35:1, and 70:1, for 1-FO, 3-FO, 5-FO, and 10-FO, respectively. It is interesting that the intensity of the green emission scales almost linearly with the amount of fluorenone incorporated in the copolymers. As the number of lower-energy fluorenone traps on the polyfluorene backbone increases, the probability of exciton localization and radiative recombination on those traps increases. The exciton diffusion to the fluorenone traps would be a three-dimensional process in copolymer thin films, whereas

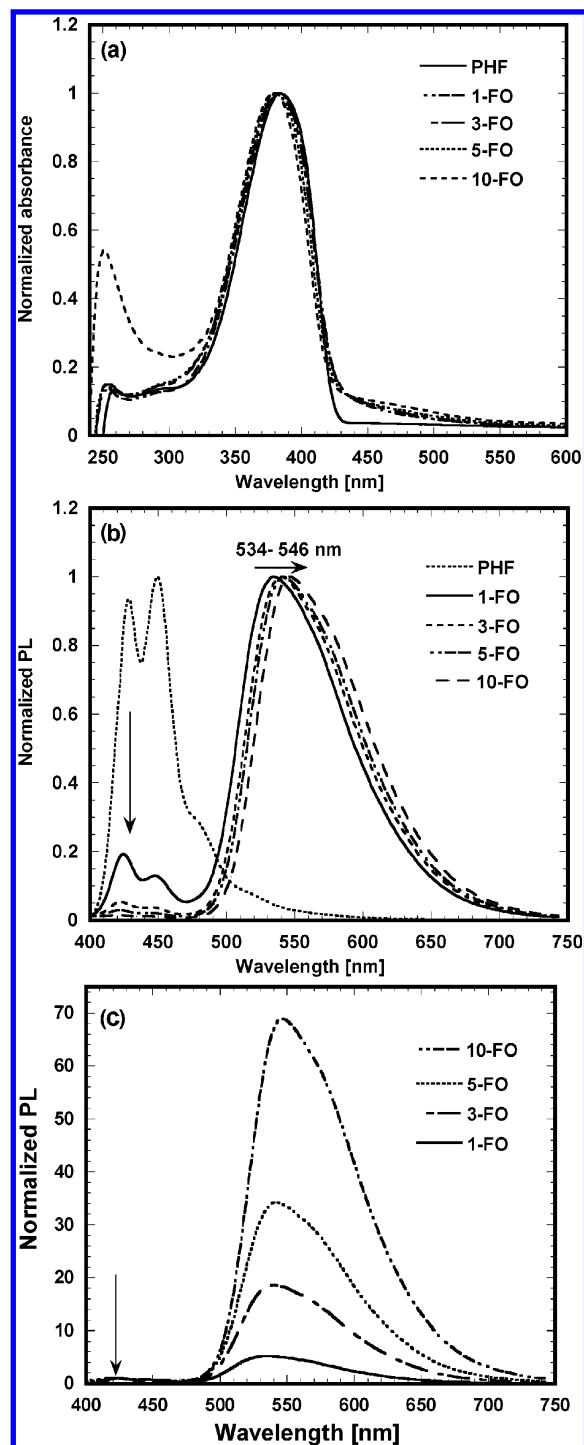


Figure 7. (a) Normalized absorption spectra of thin films of PHF and fluorenone copolymers. (b) PL emission spectra of thin polymer films, normalized relative to their respective dominant peak. (c) PL emission spectra of fluorenone copolymer thin films, normalized relative to the blue emission at 424 nm, as indicated by the arrow. The excitation wavelength was 380 nm.

it would be predominantly one-dimensional in dilute solutions. Thus, the green emission is less intense than the blue emission in all dilute fluorenone copolymer solutions, as previously shown in Figure 4b, whereas in all copolymer thin films, the green emission is the dominant one.

Time-Resolved Photoluminescence Decay Dynamics. All the results from steady-state PL emission spectra discussed so far suggest that the green emission from the fluorenone sites in the copolymers is not an aggregate emission and that intermo-

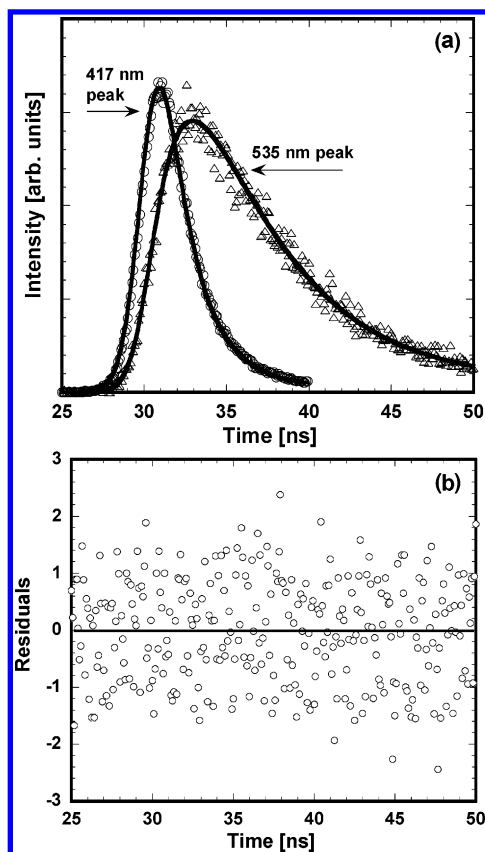


Figure 8. (a) Fluorescence decay curves of the blue and green emission peaks of 5-FO in 10^{-6} M toluene solution with 381-nm excitation. Open symbols represent the actual data and the solid lines are single-exponential fits to the data. (b) Plot of weighted residuals for the fit corresponding to the 535-nm decay curve.

lecular interactions significantly enhance it. To further shed light on the nature of the emission from fluorenone-containing polymers, we have investigated the fluorescence decays of the PL emission bands in solutions and thin films of the copolymers and the model compound BFF. Single exponential fits to the decays would indicate only one emitting monomeric species, whereas multiexponential decays would imply complex kinetics of monomeric species and excimer or aggregated complexes.¹⁰ In dilute solution (10^{-6} M), the decay of the blue emission at 416 nm was found to be single exponential with typically short lifetimes of <400 ps for all the polymers, suggesting that the emission comes from singlet intrachain excitons, as previously found for polyfluorene homopolymers.⁹ On the other hand, the green emission at 535 nm for all fluorenone copolymers had a much longer lifetime of ~ 5 ns and was also best described by a single exponential. Representative decay curves of 5-FO in toluene (10^{-6} M), with the corresponding exponential fits, are shown in Figure 8a, along with the plot of weighted residuals for the fit (Figure 8b). A summary of the time-resolved PL decay parameters in dilute solution is presented in Table 2.

The observed long lifetimes of the green emission band in the copolymers are similar to those previously reported for the 9-fluorenone molecule.¹² However, there is debate in the fluorenone photophysics literature regarding the nature of the PL emission, because the photophysics of fluorenone is extremely sensitive to the polarity of the solvent, because of the carbonyl bridge.¹² The PL emission of 9-fluorenone varies from 490 nm in nonpolar toluene to 520 nm in polar acetonitrile, with relatively long single-exponential lifetimes of 3.0 and 18.7 ns, respectively.^{12b,c} We note that the PL emission of the model

TABLE 2: Fluorescence Decay Parameters and Fluorescence Quantum Yields of the Polymers and Model Compound in 10^{-6} M Toluene Solutions

compound	λ_{exc} (nm) ^a	λ_{em} (nm) ^b	τ (ns) ^c	χ^2	DW ^d	ϕ_f (%)
PHF	381	416	0.357	1.008	1.733	100
PHF	381	535	4.819	0.962	2.435	
1-FO	381	416	0.372	1.253	1.753	98
1-FO	381	535	5.186	1.092	2.227	
3-FO	381	416	0.353	1.058	1.758	77
3-FO	381	535	5.10	1.153	1.738	
5-FO	381	416	0.373	1.054	1.947	47
5-FO	381	535	5.22	0.832	2.176	
10-FO	381	416	0.239	1.101	2.051	29
10-FO	381	535	5.017	0.956	2.114	
BFF	358	390	1.101	0.970	2.082	19
BFF	358	535	5.981	1.002	1.868	

^a Excitation wavelength. ^b Monitored emission wavelength. ^c Fluorescence lifetime extracted from the single-exponential fits. ^d Durbin–Watson parameter for the fits.

TABLE 3: Fluorescence Decay Parameters of the Polymer Thin Films

compound	λ_{exc} (nm) ^a	λ_{em} (nm) ^b	τ (ns) ^c	χ^2	DW ^d
PHF	381	428	0.405	2.423	0.890
1-FO	381	424	0.362	0.887	2.213
1-FO	381	534	6.751	1.124	1.855
3-FO	381	424	0.677	0.922	2.041
3-FO	381	539	6.305	1.104	1.942
5-FO	381	424	0.423	1.082	1.812
5-FO	381	542	5.497	1.21	2.278
10-FO	381	546	4.718	1.072	1.91

^a Excitation wavelength. ^b Monitored emission wavelength. ^c Fluorescence lifetime extracted from the single-exponential fits. ^d Durbin–Watson parameter for the fits.

compound BFF in acetonitrile was also red-shifted to 570 nm, compared to 535 nm in toluene (Figure 6a), indicative of a strongly polar emissive excited state, associated with the carbonyl bridge of the fluorenone ring. In toluene solution, the lifetime of the blue emission of BFF was 1.1 ns, whereas the lifetime of the 535-nm green band was 6 ns (Table 2). However, in acetonitrile, the lifetime of the green emission of BFF was shortened to 3 ns (not shown in Table 2), whereas the lifetime of the blue band was similar to that in toluene. The PL quantum yield of BFF in acetonitrile was approximately half of the 19% observed in toluene. From the PL decay dynamics of all copolymers and the model compound in dilute solution, we thus conclude that the green emission band in the fluorenone copolymers originates from the fluorenone units contained on single polymer chains.

The PL decay dynamics in thin films of these fluorenone-containing polymers are especially relevant, because the probability of excimer formation, if any, is highest in the solid state, compared to dilute solution. Surprisingly, a very similar trend in lifetimes was also observed for the thin-film emission of the materials, as summarized in Table 3. The blue emission at 424 nm was short-lived, with a lifetime of <700 ps, and single exponential, whereas the green emission had a much longer lifetime. The lifetime of the green emission band was 6.75, 6.30, 5.50, and 4.72 ns for 1-FO, 3-FO, 5-FO, and 10-FO, respectively. More importantly, the decay of the green emission was a single exponential in all fluorenone copolymers, implying the presence of only one type of emitting species, which would not be expected for typical excimer emission in thin films.¹⁰

The similarity of the lifetimes of the copolymer emission in solution and thin film to those of BFF suggests that BFF is a good representation of the actual chromophore responsible for the green emission in the copolymers. Furthermore, the single-exponential PL decay of the 535-nm emission and the similarity of the PL lifetimes of fluorenone copolymers to BFF suggest that the green emission originates from on-chain monomeric fluorenone defects, rather than intermolecular excimers of fluorenone.

We note that there have been debatable reports on excimer emission from the 9-fluorenone molecule itself in concentrated solutions.^{12e,f} Emission from 9-fluorenone excimers, presumably formed by a triplet–triplet annihilation process, was proposed.^{12e,f} However, the reported “monomer” lifetimes of 10.36 and 9.66 ns in benzene and acetonitrile, respectively, and “excimer” lifetimes of 4.90 and 8.83 ns, respectively, do not agree with the widely accepted fluorescence lifetimes (3.0 ± 0.2 ns in toluene and 18.7 ± 0.7 ns in acetonitrile) of 9-fluorenone.^{12b,c} The hypothesis for intermolecular excimer origin of the green emission band in fluorenone-containing polyfluorenes was based on the prior reports of excimer emission in 9-fluorenone solutions.^{8b} In addition to prior evidence against excimer formation in 9-fluorenone solutions, our results rule out excimers as the origin of the 535-nm emission band in BFF, which is the more relevant model compound for fluorenone-containing polyfluorenes. Regarding the controversy over the origin of the additional green band in blue-emitting polyfluorenes,¹³ recent reports claim that it is a single-chain defect emission from the fluorenone moieties and not an aggregate or excimer emission.^{6c–e} However, to the best of our knowledge, systematic analysis of the PL decay dynamics of model fluorenone-incorporated copolymers and a suitable model compound has been lacking so far. Therefore, the present detailed fluorescence lifetime data provide crucial evidence in support of the single-chain fluorenone defect emission hypothesis and against the intermolecular excimer model of the green emission band.

Effects of Intermolecular Interactions on the Green Emission. Based on all the results discussed so far, we have concluded that the controversial green emission band in polyfluorenes is not due to aggregates or excimers, but is an emission from fluorenone moieties on single polymer chains. The effective chromophore that causes the 535-nm emission band is a trimer oligofluorene with a middle fluorenone ring, i.e., BFF. The combination of our observations of the green emission band in dilute solutions of the fluorenone-containing copolymers and oligomer, the single-exponential description of the PL decay dynamics of solutions and thin films, and the similarity of the fluorescence lifetimes of the copolymers to that of the trimer oligofluorene (BFF) and 9-fluorenone provide definite evidence for the hypothesis that the green emission originates from fluorenone defects on single chains of polyfluorenes.

We now discuss the reasons why efficient green emission is obtained from the copolymers that contain such small fractions of fluorenone moieties. Previous theoretical studies of fluorenone-containing oligofluorenes proposed efficient Forster energy transfer to the fluorenone defects and strong exciton confinement on the fluorenone moieties, because of their lower-lying energy levels, compared to fluorene segments.⁷ Efficient funneling of excitation energy from the high-energy fluorene segments to the low-energy fluorenone defects results from energy migration by hopping of excitations along a single polymer chain until they are trapped on the fluorenone defects on that chain or transferred onto neighboring chains by Forster-type interchain energy transfer process. In the solution state,

the polymer chains can adopt different conformations and possess certain rotational freedom.¹⁴ In dilute solutions (10^{-7} – 10^{-6} M), one can envisage isolated chains with very limited collisions between them, and thus the energy migration would be one-dimensional by means of “loop” transfer or “non-nearest neighbor” transfer¹⁴ to the keto defects, with very little contribution from interchain energy transfer. In more concentrated solutions (10^{-4} M), the number of chain collisions would increase and interchain energy transfer would contribute to the excitons localized on fluorenone defects. Hence, we see a steady increase in the green emission at 535 nm with increase in solution concentration for all copolymers (Figure 5) and the oligomer BFF (Figure 6b). This is similar to the common “antenna effect” in energy migration studies in polymers¹⁴ with a small number of low-energy traps on the chains. In the case of the oligomer BFF in solution, one may argue whether intermolecular interactions would be as strong as those in the long-chain polymers. However, given the smaller size of the oligomer, it would have a much higher diffusion coefficient in solution than the polymer, leading to increased molecular collisions among BFF molecules and making collisional energy transfer more dominant. In addition, the lifetime of the singlet exciton on the fluorene unit (390-nm emission) in BFF at 1.1 ns is much longer, compared to the corresponding lifetimes of <400 ps in the polymers (Table 2). Thus, within the lifetime of the exciton, the probability of excitation transfer from one BFF molecule to the fluorenone unit on another molecule during their frequent collisions is much higher. Hence, as the solution concentration of BFF increases, we see a progressive increase in the green emission band at 535 nm (see Figure 6b).

In the solid state, interchain interactions are at their greatest whereas the rotational freedom of polymer chains is greatly reduced. Thus, now the energy funneling occurs in all three dimensions,^{6d} and the exciton diffusion to the fluorenone sites is enhanced by the increased interchain interactions. Thus, the dominant emission in thin films of the fluorenone copolymers is green instead of blue, unlike in solution where both the blue and green emission are observed (Figure 7b). We note that, although the 535-nm green emission band in the PL and EL spectra of polyfluorenes is significantly enhanced by the strong intermolecular interactions in thin films, this should not be interpreted as evidence of intermolecular aggregate or excimer emission. The enhancement can be fully understood in terms of the more efficient excitation energy transfer from fluorene segments to fluorenone moieties in the solid state.

Given that several prior approaches to stabilize the blue emission from polyfluorenes were premised on eliminating aggregate or excimer emission by reducing intermolecular interactions, our present results and conclusions about the green emission band raise questions about the underlying mechanisms of those approaches. Dendronization^{5e} and addition of bulky side groups^{5a,b} have been shown to successfully stabilize the blue emission of polyfluorenes by effectively reducing interchain interactions. We have also previously shown that stable blue LEDs can be obtained from binary blends of poly(9,9-dioctylfluorene) with either polystyrene or poly(vinylidenediphenylquinoline) (PVQ).^{5f} Although dendronization and blending can result in a reduction in excitation energy transfer to *existing* green-emitting fluorenone sites, they would not completely eliminate the green emission band, which is present even in dilute solutions of our fluorenone-containing polyfluorenes. To the extent that dendronization, the addition of bulky side groups, blending, or any other method has successfully eliminated the green emission band while stabilizing the blue emission in

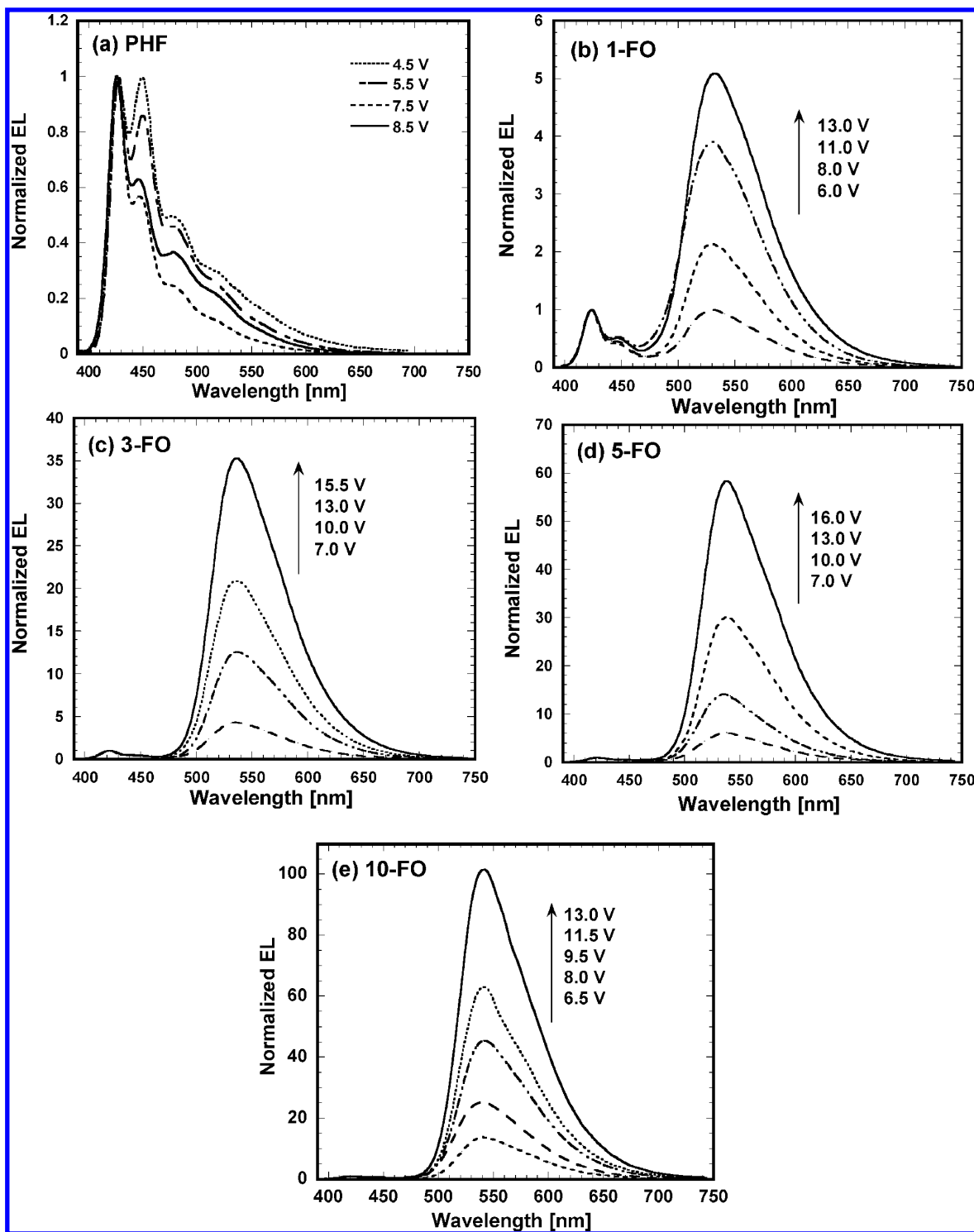


Figure 9. Normalized EL spectra of single-layer LEDs of the type ITO/PEDOT/polymer/Al: (a) PHF, (b) 1-FO, (c) 3-FO, (d) 5-FO, and (e) 10-FO.

polyfluorenes, it must be via the prevention of the photo-/electro-oxidation that produces the fluorenone defects. The detailed mechanism of how fluorenone defects are formed in polyfluorene chains is not currently understood. Calcium-catalyzed electro-oxidation, which creates fluorenone defects in polyfluorene devices with a calcium cathode, was recently proposed.¹⁵ However, the broad green emission and, hence, fluorenone defects are known in devices with aluminum cathodes.^{3a,5f,6c}

Electroluminescence. The electroluminescence (EL) properties of the fluorenone copolymers were investigated using single-layer light-emitting diodes (LEDs) comprised of indium-tin

oxide (ITO) anode, coated with a film of poly(3,4-ethylenedioxythiophene) doped with poly(styrenesulfonate) (PEDOT), and aluminum cathode. The EL spectra, normalized relative to the blue emission band, of such single-layer of PHF homopolymer and the fluorenone copolymers are shown in Figure 9. The pure blue emission of PHF is shown in Figure 9a, where the spectra are normalized relative to the 427-nm peak. At the lower voltages (4.5 and 5.5 V), the EL spectra of PHF diodes show two clear peaks at 427 and 448 nm, similar to the thin-film PL emission spectra. The clear vibronic peak at 448 nm becomes a weak shoulder at higher voltages. The EL spectra of all the

fluorenone copolymers show a very distinct evolution with increasing applied voltage. The EL spectra of 1-FO shown in Figure 9b have two main bands: one at 424 nm and the other at 532 nm. There is a clear indication of an increase in the green peak at ~ 532 nm with increasing bias voltage or electric field. At the 6.0 V turn-on voltage, the intensity of the green peak (532 nm) and blue peak (424 nm) are equal. At 13.0 V, the green peak is ~ 5 times as intense as the blue peak and closely matches the thin-film PL emission (Figure 7c). A similar trend is observed in the EL spectra of the other copolymers, as shown in parts c–e of Figure 9. In the thin-film PL emission of 3-FO, the green peak at 535 nm is ~ 18 times more intense than the blue peak (Figure 7c). Figure 9c shows that, at lower voltages, the green peak is not very intense, whereas at the higher voltages, the green peak becomes ~ 36 times more intense than the blue peak at 423 nm. The 5-FO thin-film PL spectrum has a green emission band that is 35 times more intense than the blue emission band (Figure 7c), whereas the EL spectra of 5-FO at higher voltages have a much more dominant contribution from the green band. In the EL spectra of 10-FO, the blue emission is almost completely quenched, whereas the green peak grows with applied bias. Note that all the spectra shown in Figure 9 for each polymer are for the same active pixel; however, exactly similar results were obtained for freshly turned-on pixels at each applied voltage.

The spectral evolution in the EL spectra of the fluorenone copolymers (Figure 9) is quite interesting. In all copolymers, we observed a progressive increase in the green emission band, relative to the blue band, as the strength of the electric fields increased. The formation of additional keto defects in the fluorenone–fluorene copolymers is a possible scenario in our studies, because all our device fabrication and characterization steps were performed in air and our devices were not sealed to protect them from ambient moisture and/or oxygen. However, in the case of 1-FO (Figure 9b), the intensity of the green emission band is only 5 times higher than that of the blue emission band, even at the maximum operating voltage of 13.0 V. This is exactly what was observed in the thin-film PL emission. Therefore, the observed increase in the green emission with bias voltage cannot be related to the generation of additional keto defects in the 1-FO copolymer during device operation. A likely explanation is the variation in charge recombination kinetics with applied voltage. Apparently, with increasing voltage, more charge recombination occurs on the fluorenone traps responsible for the green emission, compared to the fluorene segments that emit blue light. It was proposed recently that the charge recombination kinetics for the blue emission from the fluorene segments and green emission from the keto defects is dependent on the electric field.^{6f} In the case of 3-FO, 5-FO, and 10-FO, the green emission in their EL is more intense than in their PL, at the higher applied voltages (Figure 9). The green emission band from the fluorenone moieties is known to be stronger in EL than in PL, because of charge carrier trapping on the keto defects, in addition to the exciton energy transfer to the defects.^{6c} As the fluorenone content in the copolymers increases, there would be increased charge trapping on such fluorenone defects, leading to pronounced green emission in EL. This explains the intense green emission band at the higher voltages in diodes made from 3-FO, 5-FO, and 10-FO.

The current density–electric field and luminance–voltage characteristics of the LEDs are shown in Figure 10. The turn-on electric field for PHF diode is ~ 1.3 MV/cm, whereas that for the copolymers is slightly higher, at ~ 1.6 – 1.8 MV/cm. The

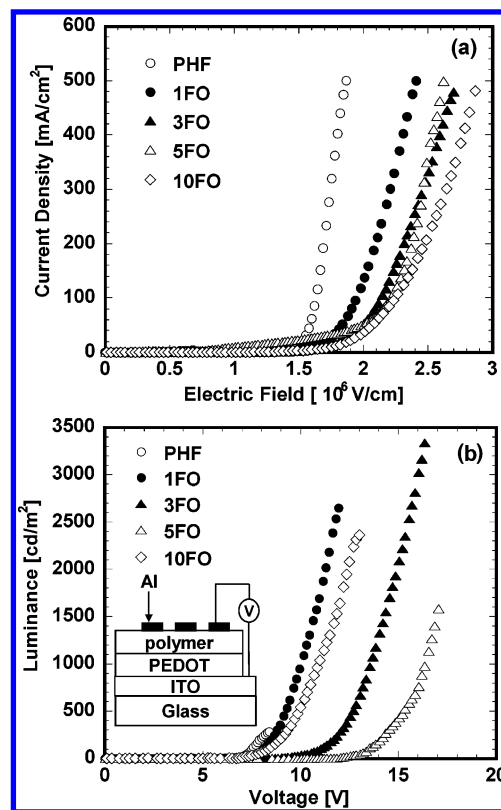


Figure 10. (a) Current density–electric field characteristics of polymer LEDs. (b) Luminance–voltage characteristics of the devices in Figure 10a; the inset shows a schematic of the device.

TABLE 4: Device Characteristics of ITO/PEDOT/Polymer/Al Light-Emitting Diodes (LEDs)

polymer	voltage (V)	current density (mA/cm ²)	brightness (cd/m ²)	EQE (%) ^a
PHF	8.4	500	280	0.07
1-FO	12.0	500	2680	0.16
3-FO	16.3	500	3340	0.19
5-FO	17.0	500	1600	0.10
10-FO	13.0	500	2360	0.15

^a External quantum efficiency, calculated at the given drive voltage, current density, and corresponding brightness.

higher turn-on electric field in the copolymer diodes, compared to PHF diodes, is to be expected, because fluorenone moieties are known to act as electron traps on the polyfluorene chains, and thus charge recombination will be delayed, compared to that observed with PHF. The current passing through the copolymer devices is much lower than that through the PHF device for the same electric field, suggesting that there is better charge recombination efficiency in the copolymers. In addition, the decrease in current density from 1-FO to 10-FO suggests higher charge trapping with increasing fluorenone content in the copolymers. Figure 10b shows the variation in brightness of the LEDs as a function of applied voltage. The PHF homopolymer LED has a brightness of 280 cd/m² and an external quantum efficiency of 0.07% at 8.4 V with a current density of 500 mA/cm². The brightness of all the copolymer LEDs is much higher than that of the PHF diode. The brightness was 2680, 3340, 1600, and 2360 cd/m² for the 1-FO, 3-FO, 5-FO, and 10-FO diodes, respectively. The corresponding external quantum efficiencies were 0.10%–0.19% and, thus, also varied with fluorenone content. The EL device characteristics are summarized in Table 4.

The variation in luminance and external quantum efficiency of the single-layer LEDs with fluorenone content in the

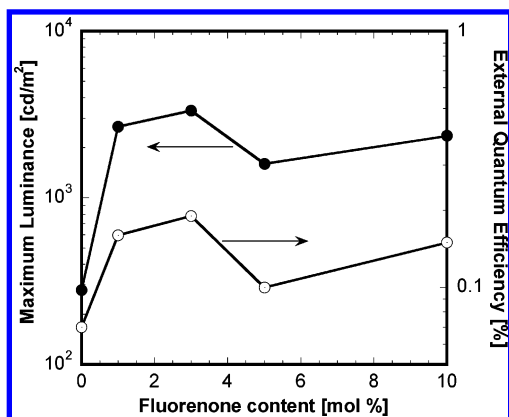


Figure 11. Semilogarithmic plot of external quantum efficiency and luminance of single-layer LEDs versus fluorenone content in the polyfluorene.

copolymer is shown in Figure 11. Although PHF has a high PL quantum yield, the EL brightness is much lower than the fluorenone copolymers, because of an imbalance in charge carrier injection and transport. These factors are significantly enhanced in the fluorenone copolymers, leading to the much improved brightness (an enhancement of ~ 6 – 12 times) in the copolymer LEDs, compared to the PHF diodes. The improved luminance and external quantum efficiency result from the better charge recombination efficiency and radiative decay in the fluorenone copolymers, where the fluorenone moieties act as electron traps and radiative decay sites on the polyfluorene chains. We note that an electron affinity as high as 3.3 eV has been reported for polyfluorenone,¹⁶ which suggests that electron injection and transport would be much improved in the fluorenone copolymers. In addition, efficient Forster energy transfer from the high-energy fluorene segments to the low-energy fluorenone sites leads to strong radiative recombination on the fluorenone defects. However, among the fluorenone copolymers, the best LED performance was obtained from 3-FO, as shown in Figure 11. These results suggest that the fluorenone–fluorene copolymers are very good candidates as robust green electroluminescent materials for LEDs.

Interestingly, although the presence of keto defects in electroluminescent arylene vinylene polymers such as poly(*p*-phenylenevinylene)s quenches the luminescence and is detrimental to LEDs,¹⁷ keto defects and thus fluorenone moieties in the polyfluorenes act as efficient guest emitters in devices, albeit at a different color. Given that the single-layer LEDs with aluminum cathodes are very basic with no additional charge-transporting layers or blend components, we believe that the brightness and efficiency achievable with the fluorenone copolymers can be significantly improved by optimizing the device geometry.

Conclusions

We have synthesized a series of four statistical copolymers of 9,9-dihexylfluorene and 9-fluorenone that contain 1%, 3%, 5%, and 10% fluorenone by Suzuki coupling polymerization and used them as model systems to investigate the photophysics and the origin of the green emission in polyfluorenes. Of particular significance is the oligofluorene trimer 2,7-bis(2'-9',9'-dihexylfluorenyl)-9-fluorenone (BFF), which is also synthesized by Suzuki coupling, whose solution photophysics simulates the green emission properties of the fluorenone-containing polyfluorenes and, thus, is an excellent model of the active green-emitting chromophore in polyfluorenes. Our steady-state PL data

in conjunction with the PL decay dynamics of all fluorenone-containing copolymers and oligomer allow us to conclude that the controversial 535-nm green emission of the polyfluorenes originates from the fluorenone defects in single-chain polymers, definitively ruling out interchain aggregate or excimer emission. The observed strong effect of intermolecular interactions on the intensity of the green emission was explained as being due to increased energy transfer efficiency in populating the fluorenone traps. Our results also suggest that some of the current methods of stabilizing the blue emission of polyfluorenes, such as dendronization and blending, likely impede the oxidation process that forms the fluorenone defects. Bright green electroluminescence (EL) was achieved from single-layer copolymer light-emitting diodes (LEDs), with brightness levels in the range of 1600–3340 cd/m². Enhanced LED performance, compared to poly(9,9-dihexylfluorene) (PHF) LEDs, was obtained as a result of improved electron injection and transport in the copolymers due to the presence of electron-deficient fluorenone moieties. These results suggest that the fluorenone–fluorene copolymers are robust green electroluminescent materials for LEDs.

Experimental Section

Characterization. The TGA and DSC thermograms were obtained (TA Instruments, models Q50 TGA and Q100 DSC, respectively) in nitrogen at heating rates of 20 and 10 °C/min, respectively. ¹H NMR spectra were taken at 300 MHz on a Bruker model AF301 spectrometer. GPC analysis of the polymers was performed on a Waters gel permeation chromatograph with Shodex gel columns and Waters model 150 C refractive index detectors at 30 °C with a THF flow rate of 0.5 mL/min. The molecular weight measurement was calibrated with polystyrene standards.

Optical Absorption and Photoluminescence Spectroscopy. Optical absorption spectra were recorded using a Perkin-Elmer model Lambda 900 UV/vis/near-IR spectrophotometer. Solution spectroscopy was performed in quartz cuvettes with a path length of 1 cm. Steady-state PL studies were conducted on a Photon Technology International (PTI), Inc. model QM-2001-4 spectrofluorimeter. In solution, the PL emission was detected in the right-angle geometry, to minimize self-absorption effects. Thin films were positioned at an angle of $\sim 22^\circ$, with respect to the excitation beam, with emission detector fixed at 90° , with respect to the excitation light. Thin films for optical absorption and PL measurements were spin-coated on glass slides from toluene solutions of polymers. All the films were dried at 60 °C, typically overnight under vacuum, to remove any residual solvent. The PL quantum yields in solution were estimated using a 10^{-5} M solution of 9,10-diphenylanthracene in toluene as a standard ($\phi_{\text{PL}} = 93\%$).¹⁸ Corrections for refractive indices of solvents were made as needed.

Time-Resolved Photoluminescence Decay Dynamics. Fluorescence decays were measured on a PTI model QM-2001-4 spectrofluorimeter that was equipped with a Strobe Lifetime upgrade. The instrument utilizes a nanosecond flash lamp as an excitation source and a stroboscopic detection system. All measurements were performed at room temperature. The decay curves were analyzed using a multiexponential fitting software package that was provided by the manufacturer. Reduced χ^2 values, Durbin–Watson parameters, and weighted residuals were used as the goodness-of-fit criteria.

Fabrication and Characterization of Light-Emitting Diodes. All the polymer LEDs were fabricated as single-layer sandwich structures between aluminum cathodes and indium–tin oxide (ITO) anodes. ITO-coated glass substrates (Delta

Technologies Ltd., Stillwater, MN; $R_s = 8\text{--}12 \text{ } \Omega/\square$) were cleaned sequentially in ultrasonic baths of detergent, a mixture of 2-propanol/deionized water (1:1 volume), toluene, deionized water, and acetone. A 75-nm-thick hole injection layer of poly(ethylenedioxythiophene) doped with poly(styrenesulfonate) (PEDOT) was coated on top of the ITO and dried at 200 °C for 15 min under vacuum. Solutions of the polymers (7–10 mg/mL in toluene) were filtered through 0.2- μm GHP Acrodisc syringe filters (Pall Gelman Laboratory) before spin coating. Thin films of the polymers were spin-coated onto the PEDOT layer and dried at 60 °C overnight under vacuum to remove residual solvent. Depending on the processing conditions, the film thicknesses obtained were in the range of 50–70 nm and were measured by an Alpha-Step 500 surface profiler (KLA Tencor, Mountain View, CA). Finally, the top contacts of 130–150-nm aluminum cathodes were thermally evaporated through a shadow mask onto the polymer films, using an Auto 306 vacuum coater (BOC Edwards, Wilmington, MA), and typical evaporations were performed at base pressures of $<2 \times 10^{-6}$ Torr. The active area of each EL device defined by the size of the aluminum contacts was 0.2 cm². EL spectra were obtained using a PTI QM-2001-4 spectrophotometer. Current–voltage characteristics of the LEDs were measured using a model HP4155A semiconductor parameter analyzer (Yokogawa Hewlett–Packard, Tokyo). The brightness was simultaneously measured using a model 370 optometer (UDT Instruments, Baltimore, MD) equipped with a calibrated luminance sensor head (model 211). The external quantum efficiencies were calculated as previously reported.^{5f} All the device fabrication and characterization steps were performed under ambient laboratory conditions.

Chemicals. 2,7-Dibromofluorene, 9,9-dihexylfluorene-2,7-bis(trimethylene boronate), 2-bromofluorene, 1-bromohexane, Aliquat 336, and tetrakis(triphenyl)phosphine palladium [Pd(PPh₃)₄] were purchased from Aldrich. The PHF homopolymer was purchased from American Dye Source, Inc., and had a molecular weight of $M_w = 45\,000$. High-purity high-performance liquid chromatography (HPLC)-grade solvents from Fisher Scientific were used as received to make the polymer solutions.

General Polymerization Procedure for Poly(9,9-dihexylfluorene-2,7-diyl-co-2,7-fluorenone). In a flask, 9,9-dihexylfluorene-2,7-bis(trimethylene boronate) (0.5023 g, 1 mmol), 2,7-dibromofluorenone and 2,7-dibromo-9,9-dihexylfluorene (total 1.0 mmol), sodium carbonate (20 mmol, 2.12 g), and 0.05 g of Aliquat 336 were dissolved in a mixture of toluene (15 mL) and water (10 mL) under argon. Pd(PPh₃)₄ (23 mg) was added. The mixture was stirred for 48 h at 100 °C and then washed with water (50 mL). The copolymer was precipitated twice from a methanol/HCl mixture (ratio of 100/1, v/v).

1-FO Copolymer. The molar ratio among 9,9-dihexylfluorene-2,7-bis(trimethylene boronate) (502.3 mg, 1.0 mmol), 2,7-dibromofluorenone (6.8 mg, 0.02 mmol), and 2,7-dibromo-9,9-dihexylfluorene (482.5 mg, 0.98 mmol) was 100/2/98. A light yellow copolymer (0.58 g, 88% yield) was obtained after drying in a vacuum oven at 60 °C. ¹H NMR (TMS, CDCl₃), δ (ppm): 7.83 (m, 2H), 7.67 (m, 4H), 2.11 (4H, 2CH₂), 1.14 (b, 12H, 6CH₂), 0.79 (b, 10H, 2CH₃, 2CH₂). FT-IR (KBr), ν (cm⁻¹): 2954, 2927, 2856, 1457, 812. GPC (THF, PSt standard): $M_n = 2.76 \times 10^4$, $M_w/M_n = 2.68$.

3-FO Copolymer. The molar ratio among 9,9-dihexylfluorene-2,7-bis(trimethylene boronate) (502.3 mg, 1 mmol), 2,7-dibromofluorenone (20.3 mg, 0.06 mmol), and 2,7-dibromo-9,9-dihexylfluorene (462.8 mg, 0.94 mmol) was 100/6/94. A

yellow copolymer (0.57 g, 87% yield) was obtained. ¹H NMR (TMS, CDCl₃), δ (ppm): 7.83 (m, 2H), 7.67 (m, 4H), 2.11 (4H, 2CH₂), 1.14 (b, 12H, 6CH₂), 0.79 (b, 10H, 2CH₃, 2CH₂). FT-IR (KBr), ν (cm⁻¹): 2954, 2927, 2856, 1457, 812. GPC (THF, PSt standard): $M_n = 2.17 \times 10^4$, $M_w/M_n = 2.26$.

5-FO Copolymer. The molar ratio among 9,9-dihexylfluorene-2,7-bis(trimethylene boronate) (502.3 mg, 1 mmol), 2,7-dibromofluorenone (33.8 mg, 0.10 mmol), and 2,7-dibromo-9,9-dihexylfluorene (443.1 mg, 0.90 mmol) was 100/10/90. A yellow copolymer (0.59 g, 91% yield) was obtained. ¹H NMR (TMS, CDCl₃), δ (ppm): 8.03 (very weak), 7.83 (m, 2H), 7.67 (m, 4H), 2.11 (4H, 2CH₂), 1.14 (b, 12H, 6CH₂), 0.79 (b, 10H, 2CH₃, 2CH₂). FT-IR (KBr), ν (cm⁻¹): 2954, 2927, 2856, 1719 (C=O), 1608, 1457, 813. GPC (THF, PSt standard): $M_n = 3.64 \times 10^4$, $M_w/M_n = 3.39$.

10-FO Copolymer. The molar ratio among 9,9-dihexylfluorene-2,7-bis(trimethylene boronate), 2,7-dibromofluorenone (67.6 mg, 0.20 mmol), and 2,7-dibromo-9,9-dihexylfluorene (393.9 mg, 0.80 mmol) was 100/20/80. A yellow copolymer (0.60 g, 95% yield) was obtained. ¹H NMR (TMS, CDCl₃), δ (ppm): 8.03 (weak), 7.83 (m, 2H), 7.67 (m, 4H), 2.11 (4H, 2CH₂), 1.14 (b, 12H, 6CH₂), 0.79 (b, 10H, 2CH₃, 2CH₂). FT-IR (KBr), ν (cm⁻¹): 2954, 2927, 2856, 1718 (C=O), 1608, 1457, 813. GPC (THF, PSt standard): $M_n = 3.35 \times 10^4$, $M_w/M_n = 3.33$.

50-FO Copolymer. The molar ratio among 9,9-dihexylfluorene-2,7-bis(trimethylene boronate) (502.3 mg, 1 mmol) and 2,7-dibromofluorenone (338 mg, 1 mmol) was 1/1. During the polymerization, a brownish solid precipitated out of solution.

2-Bromo-9,9-dihexylfluorene. 2-Bromofluorene (4.90 g, 20 mmol) was reacted with 1-bromohexane in a solution of potassium hydroxide (4.49 g, 80 mmol) in dimethylsulfoxide (DMSO)/H₂O (50 mL/5 mL) at room temperature under argon for 12 h. The mixture was washed with water (100 mL \times 2) and extracted with 100 mL of methylene chloride. The organic layer was dried over MgSO₄. The crude product was purified by flash chromatography (with hexane as the eluent) and gave 7.03 g (85% yield) of liquid product. ¹H NMR (TMS, CDCl₃), δ (ppm): 7.66 (m, 1H, Ar-H), 7.53 (d, 1H Ar-H), 7.45 (m, 2H, Ar-H), 7.32 (d, 3H, Ar-H), 1.92 (m, 4H, CH₂), 1.04 (m, 12H, CH₂), 0.76 (t, 6H, CH₃), 0.59 (m, 4H, CH₂).

9,9-Dihexylfluorenyl-2-boronic acid. To a solution of 2-bromo-9,9-dihexylfluorene (4.13 g, 10 mmol) in 50 mL of THF at -78 °C, butyllithium (6 mL, 12 mmol, 2.0 M in cyclohexane) was added dropwise. The mixture was stirred at -78 °C for 1 h, and then trimethyl boronate (1.35 mL, 12 mmol) was added. The mixture was warmed to room temperature and stirred overnight. After hydrolysis by adding 50 mL of 2 M HCl for 30 min, the organic layer was washed with brine and dried over MgSO₄. The solvent was removed, and the residue was purified by flash column chromatography on a silica gel with a hexane/ethyl acetate mixture (ratio of 2/1) as the eluent, to afford 2.3 g (61% yield) of white precipitate. ¹H NMR (TMS, CDCl₃), δ (ppm): 8.31 (m, 1H, Ar-H), 8.22 (s, 1H), 7.89 (d, 1H), 7.81 (m, 1H), 7.38 (m, 3H), 2.05 (m, 4H), 0.97–1.22 (m, 12H), 0.77 (t, 6H, 2CH₃), 0.68 (m, 4H).

2,7-Bis(2'-9',9'-dihexylfluorenyl)-9-fluorenone (BFF). In a flask, 2,7-dibromofluorenone (0.169 g, 0.5 mmol), 9,9-dihexylfluorene-2-boronic acid (0.946 g, 2.5 mmol), sodium carbonate (20 mmol, 2.12 g) and 0.05 g of Aliquat 336 was dissolved in a mixture of toluene (15 mL) and water (10 mL) under argon. Pd(PPh₃)₄ (23 mg) was added. After stirring overnight at 100 °C, the mixture was extracted with methylene chloride (50 mL), and washed with water (50 mL). The organic phase was dried over anhydrous MgSO₄. After removing the solvent, the residue

was purified by silica gel chromatography with a ether/hexane mixture (ratio of 1/9, v/v). A red powder (0.40 g, 94% yield) was obtained. IR (KBr pellet), ν (cm⁻¹): 2928, 2856, 1718 (C=O), 1604, 1448, 825, 740. ¹H NMR (CDCl₃), δ (ppm): 8.03 (d, 2H, ArH), 7.84–7.72 (m, 6H, Ar–H), 7.65–7.60 (m, 6H, Ar–H), 7.36 (m, 6H, Ar–H), 2.02 (m, 8H, CH₂), 1.07 (m, 24H, CH₂), 0.76 (t, 12H, CH₃), 0.68 (m, 8H).

Acknowledgment. This research was supported by the U.S. Army Research Office TOPS MURI Program (Grant No. DAAD19-01-1-0676) and the U.S. Army Research Office DURINT Program (Grant No. DAAD19-01-1-0499).

References and Notes

- (1) Recent reviews on polymer electroluminescence: (a) Friend, R. H.; Gymer, R. W.; Holmes, A. B.; Burroughes, J. H.; Marks, R. N.; Taliani, C.; Bradley, D. D. C.; Dos Santos, D. A.; Brédas, J. L.; Lögdlund, M.; Salaneck, W. R. *Nature* **1999**, *397*, 121–128. (b) Bernius, M. T.; Inbasekaran, M.; O'Brien, J.; Wu, W. *Adv. Mater.* **2000**, *12*, 1737–1750. (c) Kraft, A.; Grimsdale, A. C.; Holmes, A. B. *Angew. Chem., Int. Ed.* **1998**, *37*, 402–428. (d) Heeger, A. J. *Solid State Commun.* **1998**, *107*, 673–679. (e) Kim, D. Y.; Cho, H. N.; Kim, C. Y. *Prog. Polym. Sci.* **2000**, *25*, 1089–1139.
- (2) (a) Hu, B.; Karasz, F. E. *J. Appl. Phys.* **2003**, *93*, 1995–2001. (b) Peng, Z.; Bao, Z.; Galvin, M. E. *Chem. Mater.* **1998**, *10*, 2086–2090. (c) Jenekhe, S. A.; Zhang, X.; Chen, X. L.; Choong, V.-E.; Gao, Y.; Hsieh, B. R. *Chem. Mater.* **1997**, *9*, 409–412. (d) Tarkka, R. M.; Zhang, X.; Jenekhe, S. A. *J. Am. Chem. Soc.* **1996**, *118*, 9438–9439. (e) Zhang, X.; Shetty, A. S.; Jenekhe, S. A. *Acta Polym.* **1998**, *49*, 52–55. (f) Zhang, X.; Shetty, A. S.; Jenekhe, S. A. *Macromolecules* **1999**, *32*, 7422–7429. (g) Zhang, X.; Jenekhe, S. A. *Macromolecules* **2000**, *33*, 2069–2082. (h) Alam, M. M.; Jenekhe, S. A. *Chem. Mater.* **2002**, *14*, 4775–4780. (i) Tonzola, C. J.; Alam, M. M.; Jenekhe, S. A. *Adv. Mater.* **2002**, *14*, 1086–1090.
- (3) Recent reviews on polyfluorenes: (a) Neher, D. *Macromol. Rapid Commun.* **2001**, *22*, 1365–1385. (b) Scherf, U.; List, E. J. W. *Adv. Mater.* **2002**, *14*, 477–487. (c) Leclerc, M. *J. Polym. Sci. Part A: Polym. Chem.* **2001**, *39*, 2867–2873. (d) Becker, S.; Ego, C.; Grimsdale, A. C.; List, E. J. W.; Marsitzky, D.; Pogantsch, A.; Setayesh, S.; Leising, G.; Müllen, K. *Synth. Met.* **2002**, *125*, 73–80.
- (4) (a) Redecker, M.; Bradley, D. D. C.; Inbasekaran, M.; Woo, E. P. *Appl. Phys. Lett.* **1998**, *73*, 1565–1567. (b) Babel, A.; Jenekhe, S. A. *Macromolecules* **2003**, *36*, 7759–7764.
- (5) (a) Ego, C.; Grimsdale, A. C.; Uckert, F.; Yu, G.; Srdanov, G.; Müllen, K. *Adv. Mater.* **2002**, *14*, 809–811. (b) Yu, W.-L.; Pei, J.; Huang, W.; Heeger, A. J. *Adv. Mater.* **2000**, *12*, 828–831. (c) Miteva, T.; Meisel, A.; Knoll, W.; Nothofer, H. G.; Scherf, U.; Müller, D. C.; Meerholz, K.; Yasuda, A.; Neher, D. *Adv. Mater.* **2001**, *13*, 565–570. (d) Zeng, G.; Yu, W.-L.; Chua, S.-J.; Huang, W. *Macromolecules* **2002**, *35*, 6907–6914. (e) Setayesh, S.; Grimsdale, A. C.; Weil, T.; Enkelmann, V.; Müllen, K.; Meghdadi, F.; List, E. J. W.; Leising, G. *J. Am. Chem. Soc.* **2001**, *123*, 946–953. (f) Kulkarni, A. P.; Jenekhe, S. A. *Macromolecules* **2003**, *36*, 5285–5296. (g) Sainova, D.; Miteva, T.; Nothofer, G.; Scherf, U.; Glowacki, I.; Ulanski, J.; Fujikawa, H.; Neher, D. *Appl. Phys. Lett.* **2000**, *76*, 1810–1812.
- (6) (a) Lemmer, U.; Heun, S.; Mahrt, R. F.; Scherf, U.; Hopmeier, M.; Siegner, U.; Göbel, E. O.; Müllen, K.; Bässler, H. *Chem. Phys. Lett.* **1995**, *240*, 373–378. (b) Bliznyuk, V. N.; Carter, S. A.; Scott, J. C.; Klärner, G.; Miller, R. D.; Miller, D. C. *Macromolecules* **1999**, *32*, 361–369. (c) List, E. J. W.; Guentner, R.; Scandiucci de Freitas, P.; Scherf, U. *Adv. Mater.* **2002**, *14*, 374–378. (d) Lupton, J. M.; Craig, M. R.; Meijer, E. W. *Appl. Phys. Lett.* **2002**, *80*, 4489–4491. (e) Romaner, L.; Pogantsch, A.; Scandiucci de Freitas, P.; Scherf, U.; Gaal, M.; Zojer, E.; List, E. J. W. *Adv. Funct. Mater.* **2003**, *13*, 597–601. (f) Lupton, J. M.; Klein, J. *Phys. Rev. B* **2002**, *65*, 193202. (g) Nikitenko, V. R.; Lupton, J. M. *J. Appl. Phys.* **2003**, *93*, 5973–5977.
- (7) (a) Zojer, E.; Pogantsch, A.; Hennebicq, E.; Beljonne, D.; Brédas, J.-L.; Scandiucci de Freitas, P.; Scherf, U.; List, E. J. W. *J. Chem. Phys.* **2002**, *117*, 6794–6802. (b) Franco, I.; Tretiak, S. *Chem. Phys. Lett.* **2003**, *372*, 403–408.
- (8) (a) Lee, J.-K.; Klaerner, G.; Miller, R. D. *Chem. Mater.* **1999**, *11*, 1083–1088. (b) Panozzo, S.; Vial, J.-C.; Kervella, Y.; Stéphan, O. *J. Appl. Phys.* **2002**, *92*, 3495–3502. (c) Scandiucci de Freitas, P.; Scherf, U.; Collon, M.; Zojer, E.; List, E. J. W. *e-Polymers* [Online] **2002**, No. 0009.
- (9) Teetsov, J.; Fox, M. A. *J. Mater. Chem.* **1999**, *9*, 2117–2122.
- (10) (a) Jenekhe, S. A.; Osaheni, J. A. *Science* **1994**, *265*, 765–768. (b) Osaheni, J. A.; Jenekhe, S. A. *Macromolecules* **1994**, *27*, 739–742. (c) Valeur, B. *Molecular Fluorescence: Principles and Applications*; Wiley-VCH: Weinheim, Germany, 2002. (d) Förster, T. *Angew. Chem., Int. Ed. Engl.* **1969**, *8*, 333–343.
- (11) Pschirer, N. G.; Byrd, K.; Bunz, U. H. F. *Macromolecules* **2001**, *34*, 8590–8592.
- (12) (a) Andrews, L. J.; Derouede, A.; Linschitz, H. *J. Phys. Chem.* **1978**, *82*, 2304–2309. (b) Biczók, L.; Bérces, T. *J. Phys. Chem.* **1988**, *92*, 3842–3845. (c) Biczók, L.; Bérces, T.; Márta, F. *J. Phys. Chem.* **1993**, *97*, 8895–8899. (d) Murphy, R. S.; Moorlag, C. P.; Green, W. H.; Bohne, C. *J. Photochem. Photobiol. A: Chem.* **1997**, *110*, 123–129. (e) Rani, S. A.; Sobhanadri, J.; Rao, T. A. P. *J. Photochem. Photobiol. A: Chem.* **1996**, *94*, 1–5. (f) Rani, S. A.; Sobhanadri, J.; Rao, T. A. P. *Spectrochim. Acta A* **1995**, *51*, 2473–2479.
- (13) Gaal, M.; List, E. J. W.; Scherf, U. *Macromolecules* **2003**, *36*, 4236–4237.
- (14) Guillet, J. *Polymer Photophysics and Photochemistry*; Cambridge University Press: Cambridge, U.K., 1985.
- (15) Gong, X.; Iyer, P. K.; Moses, D.; Bazan, G. C.; Heeger, A. J.; Xiao, S. S. *Adv. Funct. Mater.* **2003**, *13*, 325–330.
- (16) Uckert, F.; Tak, Y.-H.; Müllen, K.; Bässler, H. *Adv. Mater.* **2000**, *12*, 905–908.
- (17) Papadimitrakopoulos, F.; Konstadinidis, K.; Müller, T. M.; Opila, R.; Chandross, E. A.; Galvin, M. E. *Chem. Mater.* **1994**, *6*, 1563–1568.
- (18) Heinrich, G.; Schoof, S.; Gusten, H. *J. Photochem.* **1974**, *3*, 315–320.